



ELSEVIER

Contents lists available at ScienceDirect



## Tetrahedron

journal homepage: [www.elsevier.com/locate/tet](http://www.elsevier.com/locate/tet)

# Stereo- and regioselective synthesis of novel $\beta$ -lactam tethered spiropyrrolizidine/pyrrolothiazole heterocyclic hybrids

Rajesh Raju <sup>a</sup>, Raghavachary Raghunathan <sup>a,\*\*</sup>, Natarajan Arumugam <sup>b,\*</sup>,  
Abdulrahman I. Almansour <sup>b</sup>, Raju Suresh Kumar <sup>b</sup>, Saeid M. Soliman <sup>c</sup>

<sup>a</sup> Department of Organic Chemistry, University of Madras, Guindy Campus, Chennai, 600 025, India

<sup>b</sup> Department of Chemistry, College of Science, King Saud University, P.O. Box 2455, Riyadh, 11451, Saudi Arabia

<sup>c</sup> Department of Chemistry, Faculty of Science, Alexandria University, P.O. Box 426, Ibrahimia, Alexandria, 21321, Egypt

## ARTICLE INFO

## Article history:

Received 21 September 2020

Received in revised form

3 February 2021

Accepted 12 February 2021

Available online 19 February 2021

## Keywords:

Spiropyrrolizidine/pyrrolothiazole  
 $\beta$ -lactam aldehyde  
Knoevenagel condensation  
1,3-Dipolar cycloaddition

## ABSTRACT

A regio- and diastereoselective synthesis of library of structurally intriguing novel hybrid heterocycles comprising spiropyrrolizidines/pyrrolothiazoles, oxindole/acenaphthenone and  $\beta$ -lactam moieties have been synthesized in good yields. The hitherto unexplored 2-((1-(4-methoxyphenyl)-4-oxo-3-phenylazetidin-2-yl)methylene) malononitriles were used as the dipolarophiles, while the dipoles were derived *in situ* from indoline-2,3-dione/acenaphthenequinone and L-proline/substituted 2-aryl-thiazolidine-4-carboxylic acids. The key step of this transformation is the 1,3-dipolar cycloaddition reaction involving the above-mentioned components offering a facile entry to biologically relevant classes of spiro heterocyclic hybrids.

© 2021 Elsevier Ltd. All rights reserved.

## 1. Introduction

Synthetic chemistry emphasizes the need to develop sustainable protocols to synthesize hybrid heterocycles possessing important biological and pharmaceutical activities [1]. Multicomponent 1,3-dipolar cycloaddition reactions are one such strategy that enables multiple chemical transformations to occur in a single-step. These reactions proceeded (i) without the need to isolate or purify the intermediates, (ii) reduction in the numbers of work-ups and (iii) minimization of extraction, thereby eliminating the usage of large quantities of volatile solvents which makes these transformations more environmentally friendly [2–5]. Besides, these strategies provide a facile route to the construction of structurally diverse complex heterocycles including hybrid spiro compounds with ease and often with excellent selectivities [6]. Spiro compounds are the key structural motifs in many natural products and biologically relevant synthetic analogs imparting unique physical and biological properties due to their exclusive three-

dimensionality that can be expected to interact more efficiently with binding pocket of target protein in biological system than flat aromatic ring system as ligand [7]. Perhaps, for this reason, the synthesis of hybrid heterocycles incorporating spiro core would be of immense interest in synthetic and medicinal chemistry.

Among them, frame works comprising spirooxindole rings attached to pyrrolidines are presented in many alkaloids and biologically relevant synthetic compounds. For instance, spirotryprostins A and B, horsfiline, elacomine, MI-219 and M – 888 have multifarious biological activities including anticancer [8], antimycobacterial [9], antimicrobial [10], anti-inflammatory, analgesic [11], local anesthetic [12] and cholinesterase inhibition activities [13]. Similarly, spiroacenaphthenone fused pyrrolidine/spiropyrrolizidine heterocyclic hybrids were reported to display interesting pharmaceutical activities such as anticancer [14], anti-inflammatory, [15] and anti-alzheimers activities [16] (Fig. 1). Hence, a progressive increase in the synthesis of spiro heterocyclic hybrids have been reported in recent literatures.

$\beta$ -Lactam is an important class of structural motif as it occurs in commonly used bicyclic  $\beta$ -lactam antibiotics such as penicillins, cephalosporins, carbapenems and carbacephem. It prevents bacterial trans peptidases from cross linking the polysaccharides cell wall [17]. Besides, monocyclic  $\beta$ -lactams have been developed for possessing a host of other interesting pharmaceutical capabilities

\* Corresponding author.

\*\* Corresponding author.

E-mail addresses: [ragharaghunathan@yahoo.com](mailto:ragharaghunathan@yahoo.com) (R. Raghunathan), [anatarajan@ksu.edu.sa](mailto:anatarajan@ksu.edu.sa) (N. Arumugam).

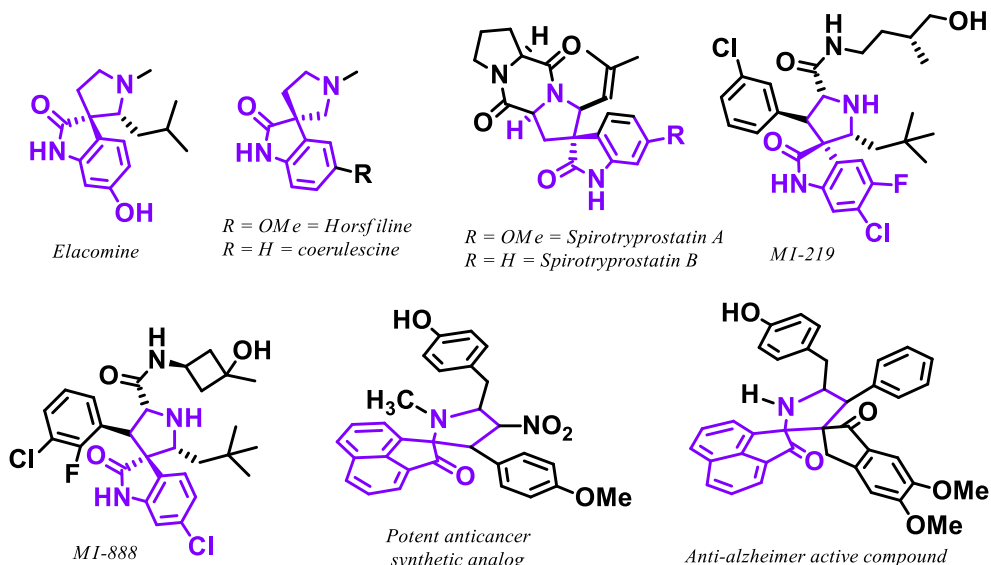


**Fig. 1.** Representative biologically relevant natural and synthetic spirooxindole and spiroacenaphthenone tethered pyrrolidine derivatives.

such as anti-HIV [18], anticancer [19,20], anti-fungal [21], anti-malarial [22], anti-inflammatory or analgesic activities [23] and play a vital role against bacterial infections over the past several decades [24].  $\beta$ -lactam is relatively high reactive structural motif due to its strained four member ring system which makes them versatile intermediates for the synthesis of functionalized  $\beta$ -amino acids,  $\beta$ -peptides, amino alcohols and chiral catalysts [25–28]. In recent past years, our research team has largely been involved in the synthesis of diverse  $\beta$ -lactam substituted heterocyclic hybrids through domino multicomponent and 1,3-dipolar cycloaddition sequence that were ultimately derived from  $\beta$ -lactam synthons which are known to possess significant biological activities [29–31].

The above mentioned biological precedents encouraged us to synthesize more novel structural hybrids comprising  $\beta$ -lactam attached with biologically active spiro heterocycles viz. spirotrytolizidines and thiazolidines in a single molecule, which would be of great interest in drug discovery. In the present study, we explored the synthesis of a novel class of heterocyclic hybrids comprising spirooxindolopyrrolizidine/pyrrolothiazole and/or spiroacenaphthenopyrrolizidine/pyrrolothiazole, and  $\beta$ -lactam employing one-pot three component 1,3-dipolar cycloaddition reaction strategy. The synthetic route for the construction of  $\beta$ -lactam substituted mono spiro heterocyclic derivatives is outlined in Fig. 2. Accordingly, structurally unknown novel class of azetidinonylmethylene-malononitrile component derived from 4-oxoazetidine-2-carbaldehyde through Knoevenagel condensation was utilized as the dipolarophile. The 1,3-dipole component, azomethine ylide derived from various substituted  $\alpha,\beta$ -diketones and secondary amino acids reacts with this unique dipolarophile affording  $\beta$ -lactam embedded mono spiroheterocyclic hybrids (Fig. 2).

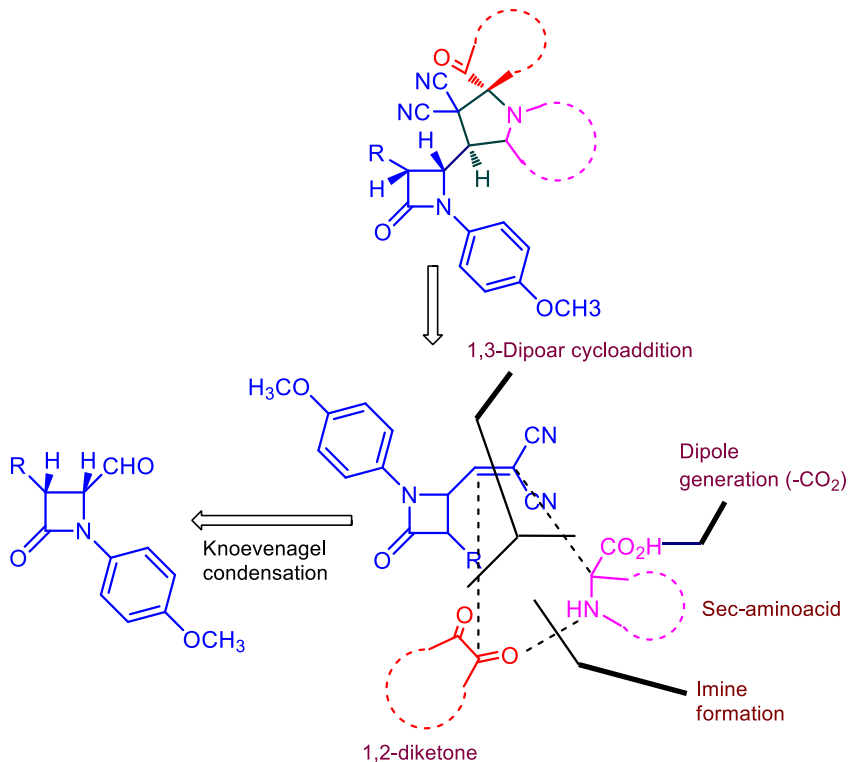
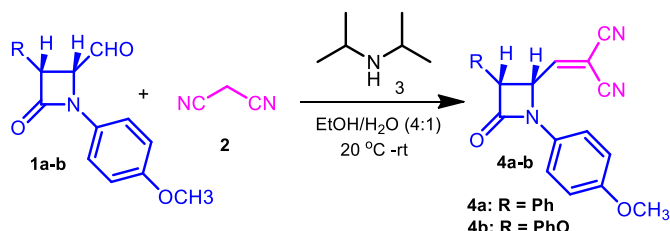
## 2. Results and discussion

The required starting substrates, 2-[(1-(4-methoxyphenyl)-4-oxo-3-phenylazetidin-2-yl)methylene]malononitriles **4** were synthesized by the Knoevenagel condensation of 4-oxoazetidine-2-carbaldehyde **1a–b** [32] and malononitrile **2** in the presence of diisopropylamine **3** as a base in a mixture of water and ethanol (1:4) at 20 °C to room temperature. Initially, the Knoevenagel

condensation was attempted with various bases such as Et<sub>3</sub>N, piperidine, pyridine, NaOH and K<sub>2</sub>CO<sub>3</sub>, no fruitful results were observed even after prolonged reaction time. Whereas, the same reaction with diisopropylamine (DIPA) in EtOH: H<sub>2</sub>O (4:1) afforded the product **4** in good yield as shown in Scheme 1. The gem-dicyano olefin segment in compounds **4a–b** acts as the active reaction site (Scheme 1).

Having synthesized 2-[(1-(4-methoxyphenyl)-4-oxo-3-phenylazetidin-2-yl)methylene]malononitrile **4a**, we then moved on to the solvent optimization for the three component 1,3-dipolar cycloaddition. The dipolarophile **4a**, isatin **5a** and L-proline **6** were selected for this optimization study. The typical reaction under reflux in various solvents viz. CH<sub>3</sub>CN, C<sub>2</sub>H<sub>5</sub>OH and CH<sub>3</sub>OH afforded the  $\beta$ -lactam tethered spirotrytolizidine heterocycle **9a** in moderate to good yields 50–85% (Table 1), while no reaction progress was observed in toluene even after prolonged reaction time. From Table 1, it was clear that methanol is the optimal solvent for this cycloaddition reaction to get maximum yield of product **9a** (85%). Then we performed the other reactions as shown in Scheme 2 employing dipolarophiles **4a–b** with isatin **5a, b** and L-proline **6** under these optimized conditions, to afford compounds **9b/10a,b** as a single product in each case, as evidenced by TLC and spectral analysis. To prove the generality of the reaction, we extended this three component reaction protocol with different substituted amino acids viz. 2-phenylthiazolidine-4-carboxylic acid **7**/2-(furan-3-yl)thiazolidine-4-carboxylic acid **8**. Thus, the azomethine ylide derived from isatin **5a,b** and secondary cyclic amino acid **7** or **8**, reacts with [(1-(4-methoxyphenyl)-4-oxo-3-phenylazetidin-2-yl)methylene]malononitriles **4** in refluxing methanol, resulting in the formation of the spiro heterocyclic hybrids **11–13** in good yield (Scheme 2, Table 2). In all these cases, a single diastereomer of the cycloadduct was obtained despite the presence of multiple stereocenters.

The structure of cycloadducts **9** and **10** was elucidated by <sup>1</sup>H and <sup>13</sup>C NMR spectroscopic techniques as illustrated for a representative example **10a**. In the <sup>1</sup>H NMR spectrum of compound **10a**, the existence of two singlets at  $\delta$  3.05 and  $\delta$  3.83 confirmed the presence of  $-NCH_3$  and  $-OCH_3$  protons. The presence of pyrrolizidine moiety was obvious from the multiplets in the region of  $\delta$  1.63–2.51, whereas the aromatic protons appeared as multiplets in the region of  $\delta$  6.78–7.65. In the <sup>13</sup>C NMR spectrum, the spiro

Fig. 2. Synthetic strategy for  $\beta$ -lactam tethered spiroheterocyclic hybridsScheme 1. Synthesis of  $\beta$ -lactam substituted dipolarophiles.

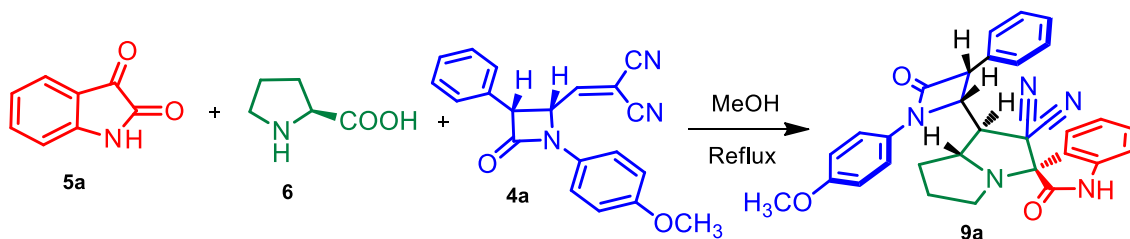
carbon displayed a peak at 77.2 ppm. The carbonyl carbons of  $\beta$ -lactam and oxindole appeared at 166.1 and 173.1 ppm respectively.

Table 1

Synthesis of **9a** with different solvents.

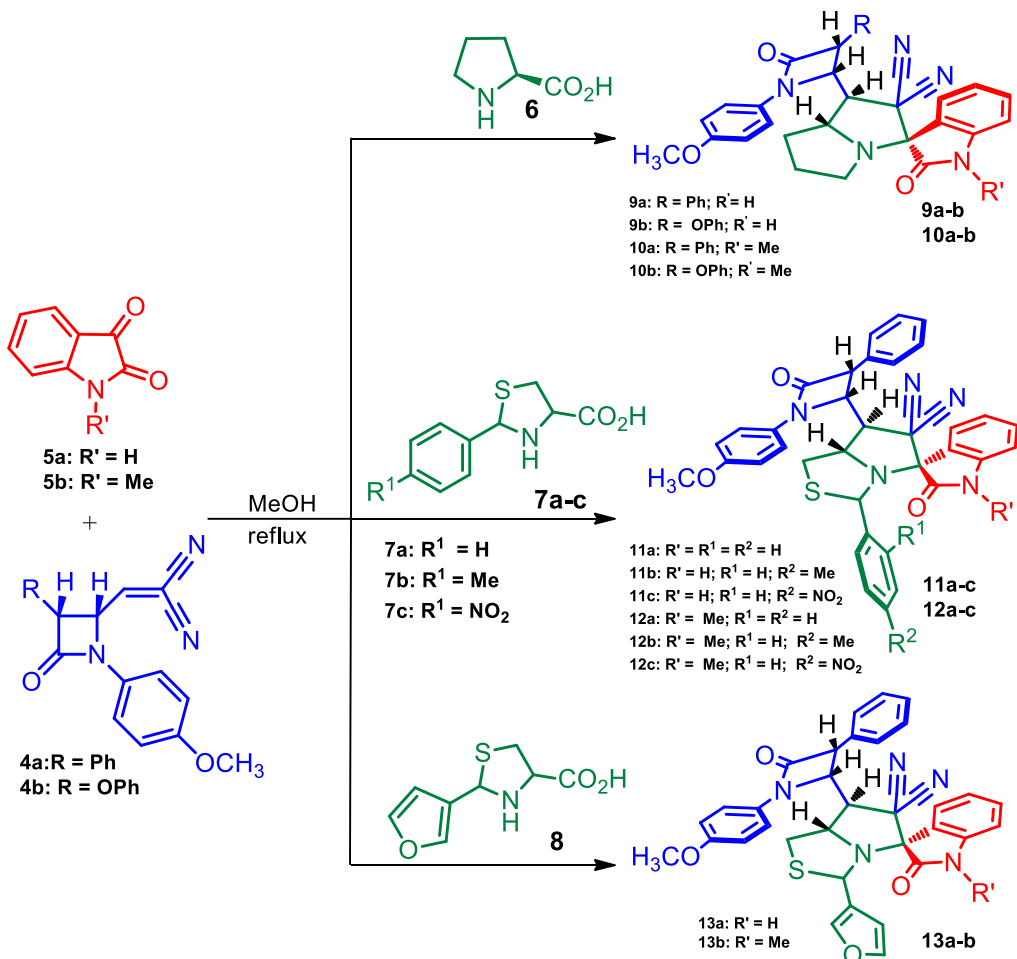
In the DEPT 135 NMR spectrum, the three peaks at 29.7, 31.2, and 48.0 in the negative region confirmed the presence of three  $-\text{CH}_2$  carbons in pyrrolizidine ring. Finally, structure of the cycloadduct **10a** was further confirmed by its single crystal X-ray analysis (Fig. 3) [33].

A reasonable mechanism to justify the formation of  $\beta$ -lactam grafted spiro heterocyclic hybrid **9–13** is depicted in Scheme 3 considering a representative case, **9a**. Initially, the Knoevenagel condensation of 4-oxoazetidine-2-carbaldehyde **1** and malononitrile **2** under basic conditions leads to the formation of **4a** via intermolecular condensation of **1** and **2**. The condensation of isatin **5a** and L-proline **6** furnished the highly reactive 1,3-dipole **17** by dehydration and decarboxylation via the



Entry	Solvents	Product	Time (h) <sup>a</sup>	Yield (%) <sup>b</sup>
1	Toluene	<b>9a</b>	18	—
2	Acetonitrile	<b>9a</b>	26	50
3	Ethanol	<b>9a</b>	10	68
4	Methanol	<b>9a</b>	5	85

<sup>a</sup> Completion of the reaction based upon TLC analysis.<sup>b</sup> Yield of isolated product after column chromatography.



**Scheme 2.** Synthesis of structurally diverse  $\beta$ -lactam tethered spirooxindolopyrrolizidines/pyrrolothiazole heterocyclic hybrids.

intermediates **15** and **16**. Subsequently, the cycloaddition of *in situ* generated 1,3-dipole **17** with the exocyclic C=C of alkene **4a**, may occur via path A or path B. However, the exclusive formation of spiropyrrolizidine **9a** reveals that path A is preferred over path B. The observed stereoselectivity in the formation of **9a** is rationalized in terms of steric consideration. Presumably, the preferential formation of **9a** is ascribable either due to the lesser unfavorable steric interaction between oxindole ring and cyanide group of **4a** or the attractive  $\pi$ - $\pi$  interaction between the CN and oxindole benzene ring via Path A. Path B, which form **18**, is not favored due to possible steric interaction between oxindole ring carbonyl and cyanide units. The regioselectivity observed in the reaction is evident from the fact that the regio isomeric product of **9a**, *viz.* **19** was not formed. This is in accord to the polarization of the C=C bond with a more electron deficient  $\beta$ -carbon in **4a** that preferentially reacts with the electron-rich carbon of the 1,3-dipole **17** affording **9a**. This cycloaddition reaction created up to five sterogenic carbons, including spiro and quaternary carbons *via* the formation of two C=C and one C=N bonds in a single pot transformation. Further, the *ortep* diagram of **10a** discloses that the oxindole carbonyl and cyanide unit are *trans*, providing a conclusive evidence to the proposed reaction pathway.

The utility of  $\beta$ -lactam dipolarophiles, **4a/b** in the construction of diverse spiroheterocyclic hybrids were further explored by performing the cycloaddition reaction with different diketone, acenaphthenequinone **20**. The cycloaddition reaction of compound **4** with acenaphthenequinone **20** and L-proline **6**/substituted

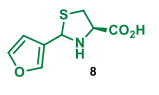
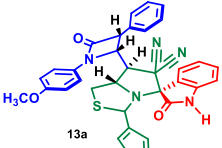
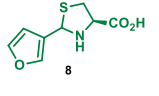
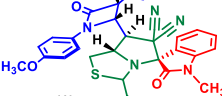
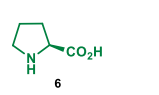
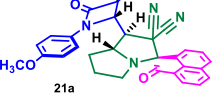
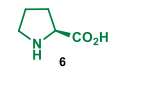
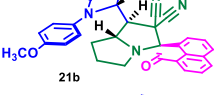
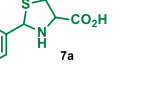
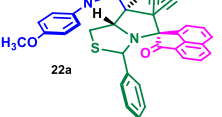
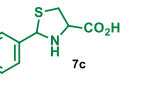
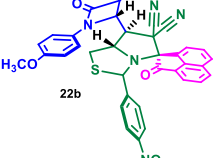
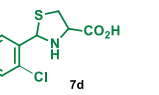
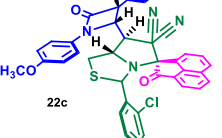
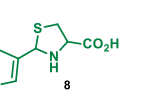
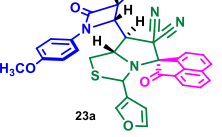
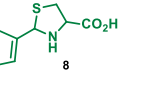
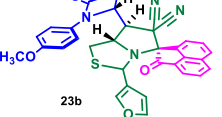
thiazolidine-2-carboxylic acids **7/8** under the optimized conditions afforded the novel spiroacenaphthenone fused pyrrolizidines **21a-b**/pyrrolothiazole hybrids **22a-c** and **23a-b** respectively (**Scheme 4**). The cycloaddition worked well with all the substrates and afforded the products in good yield (**Table 2**). The structure of all the spiro heterocycles **21a-b**, **22a-c** and **23a-b** were elucidated by adopting similar NMR chemical shift assignment as done for **10a**. Further, the stereochemistry of these spiroheterocyclic hybrids was unambiguously assigned by single crystal X-ray diffraction analysis of **22c** (**Fig. 4**) [34].

### 2.1. Hirshfeld analysis of molecular packing

The molecular packing of the synthesized compound **22c** has been analyzed using Hirshfeld surface analysis (**Fig. S1**, supplementary data). The topology analyses were performed using Crystal Explorer 17.5 program [35]. The study disclosed the different intermolecular contacts along with their percentages in the crystal structure of **22c** (**Fig. S2**, supplementary data). As can be seen from this figure, the H···H, C···H, N···H and O···H are the most dominant contacts. Their contributions are 42.5, 17.7, 12.3 and 10.8% from the whole fingerprint area (**Fig. S3**, supplementary data). Other contacts such as Cl···H (5.4%), S···H (5.3%) and C···C (3.7%) have less contribution. Among the whole observed intermolecular interactions, the Cl···H, N···H and O···H interactions are the most significant. These interactions appeared as red regions in the corresponding  $d_{\text{norm}}$  map indicating their significance (**Fig. 5**). The

**Table 2**Synthesis of angularly fused  $\beta$ -lactam substituted spirooxindolo/acenaphtheno pyrrolizidine/thiopyrrolizidine derivatives.

Entry	Precursor	1,2-diketone	sec-cyclic amino acid	Product	Time (h) <sup>a</sup>	Yield (%) <sup>b</sup>
1	4a	5a	6	9a	5.5	85
2	4b	5a	6	9b	7.0	87
3	4a	5b	6	10a	6.5	86
4	4b	5b	6	10b	8.0	83
5	4a	5a	7a	11a	6.0	85
6	4a	5a	7b	11b	5.5	84
7	4a	5a	7c	11c	7.0	87
8	4a	5b	7a	12a	6.0	84
9	4a	5b	7b	12b	8.0	85
10	4a	5b	7c	12c	7.5	87
... to be continued						

Entry	Precursor	1,2-diketone	sec-cyclic amino acid	Product	Time (h) <sup>a</sup>	Yield (%) <sup>b</sup>
11	4a				7.0	86
12	4a				8.0	84
13	4a				8.0	82
14	4b				6.5	84
15	4a				8.0	84
16	4a				7.5	86
17	4a				8.0	83
18	4a				6.5	84
19	4b				7.5	85

<sup>a</sup>Completion of the reaction based upon TLC analysis<sup>b</sup>Yield of isolated product after column chromatography

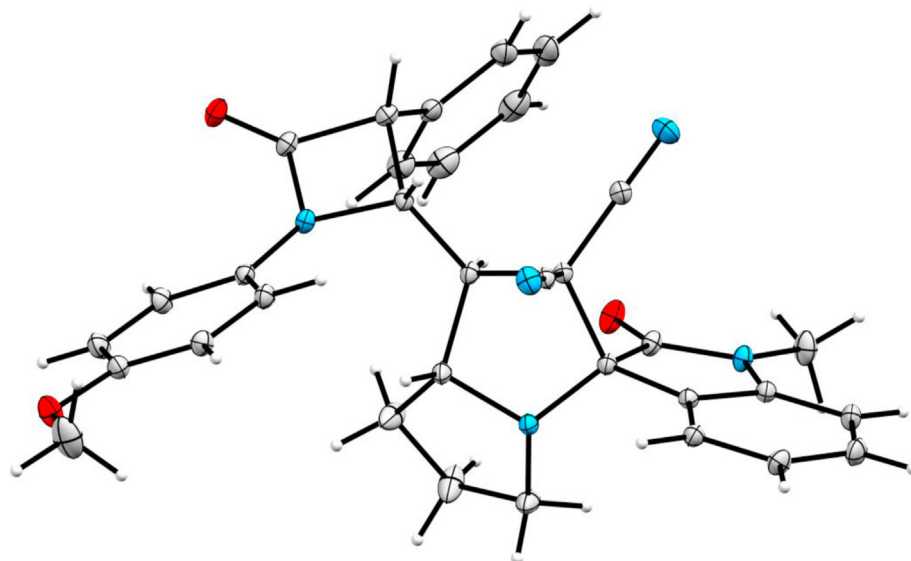


**Fig. 3.** X-ray structure of compound **10a**.

shortest contacts are N4···H7 (2.482 Å), O1···H1 (2.528 Å), O1···H19A (2.439 Å), O2···H25 (2.543 Å) and Cl1···H1A (2.812 Å) interactions with distances are generally less than the van der Waals radii sum of the interacting atoms.

## 2.2. Density functional theory studies (DFT studies)

The X-ray structure of **22c** is optimized and the calculated molecular geometry is in good agreement with the experimental data (Fig. 6). The DFT calculations were performed using Gaussian 09 software package [36] utilizing B3LYP/6-31G(d,p) method. The calculated bond distances and angles showed good agreement with the experimental data (Table S1, Supplementary data). Also, these geometric parameters provided good straight-line correlations ( $R^2 = 0.971\text{--}0.992$ ) with the experimental results as shown in Fig. 7. Small deviations could be attributed to the known fact that the calculated structure is for a single molecule in gas phase which is free from the molecular packing effects.

In addition, the calculated charges at the different atomic sites are listed in Table S2 (Supplementary data). The O (-0.580 and -0.519 e) sites have the highest negative partial charges. Also, the nitrile nitrogen atoms have negative partial charges (-0.278 and -0.273 e) which are less negative than the heterocyclic nitrogen sites (-0.552 and -0.471 e). Also, most of carbon atoms are electronegative except those attached to N or O sites. The hydrogens (0.204–0.285 e) and sulphur atom (0.212 e) have the most positive partial charges (+0.517 e). Distribution of electron density mapped over electrostatic potential (MEP) revealed these results (Fig. 8). The calculated dipole moment is high (7.027 Debye) indicating the high polarity of the compound where the direction of the dipole moment vector is towards the C=O of the four membered ring. The molecular orbital(MO) calculations predicted that the highest occupied MO is localized over the thiazole ring system while the lowest unoccupied MO is located over the naphthyl moiety and the fused five membered ring attached to it.

## 2.3. NBO analysis

In addition, natural bond orbital (NBO) analysis was used to analyze the different electron delocalization processes which stabilize the molecular systems where **22c** is taken as an example. For

this task, NBO 3.1 program [37] as implemented in the Gaussian 09W package was used. Many  $\sigma\text{-}\sigma^*$ ,  $n\rightarrow\sigma^*$ ,  $\pi\rightarrow\pi^*$  and  $n\rightarrow\pi^*$  intramolecular charge transfer (ICT) interactions stabilized its structure. The stabilization energies ( $E^{(2)}$ ) of these ICTs are calculated based on the second order perturbation theory [38,39] and the results are tabulated in Table S3, supplementary data. It is clear that the  $\sigma\text{-}\sigma^*$  and  $\pi\rightarrow\pi^*$  ICTs are the weakest where the maximum stabilization energy ( $E^{(2)}$ ) is 7.89 and 21.73 kcal/mol, respectively. In addition, the  $n\rightarrow\pi^*$  and  $n\rightarrow\sigma^*$  ICTs stabilized the system up to 54.47 and 29.61 kcal/mol, respectively.

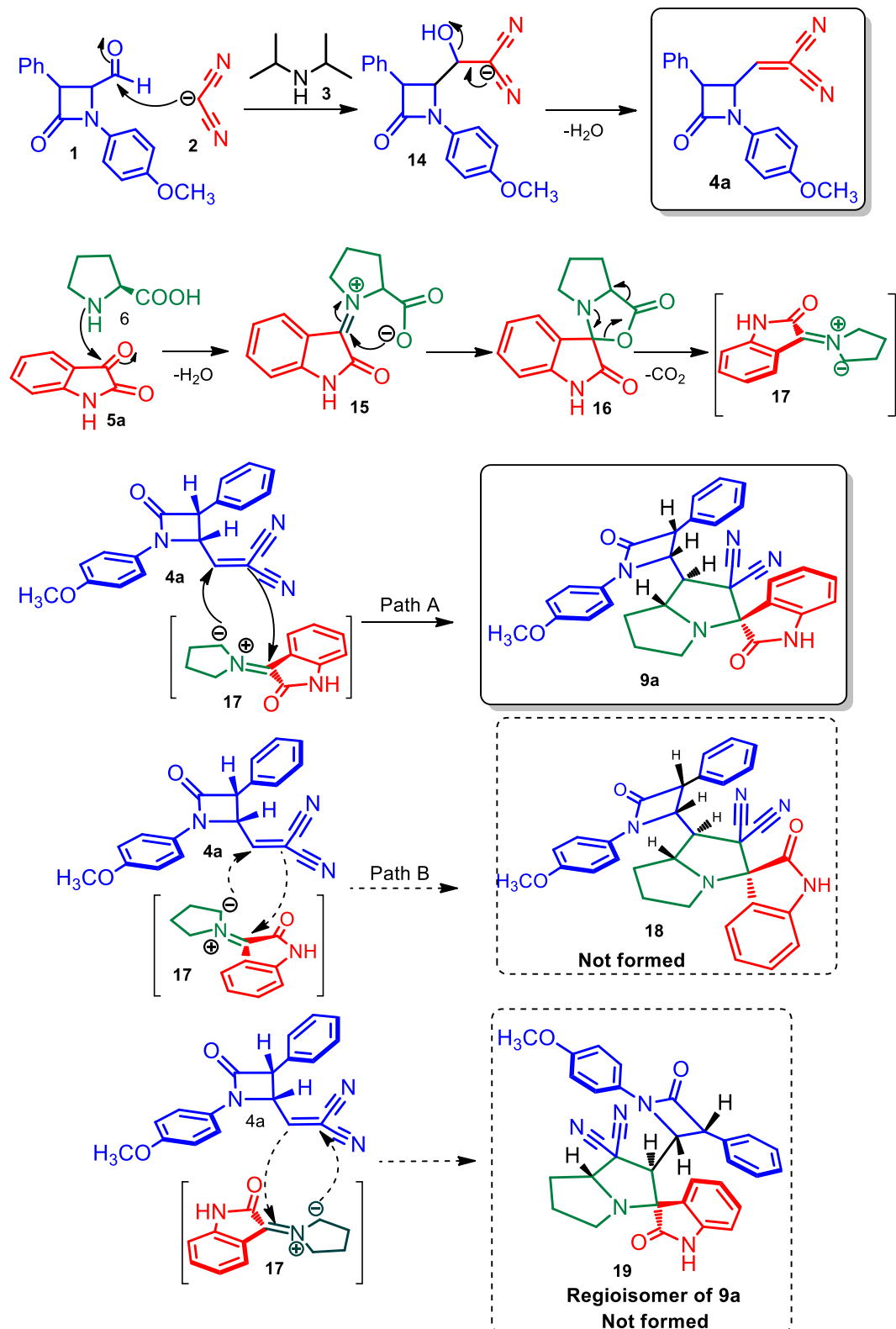
## 3. Conclusion

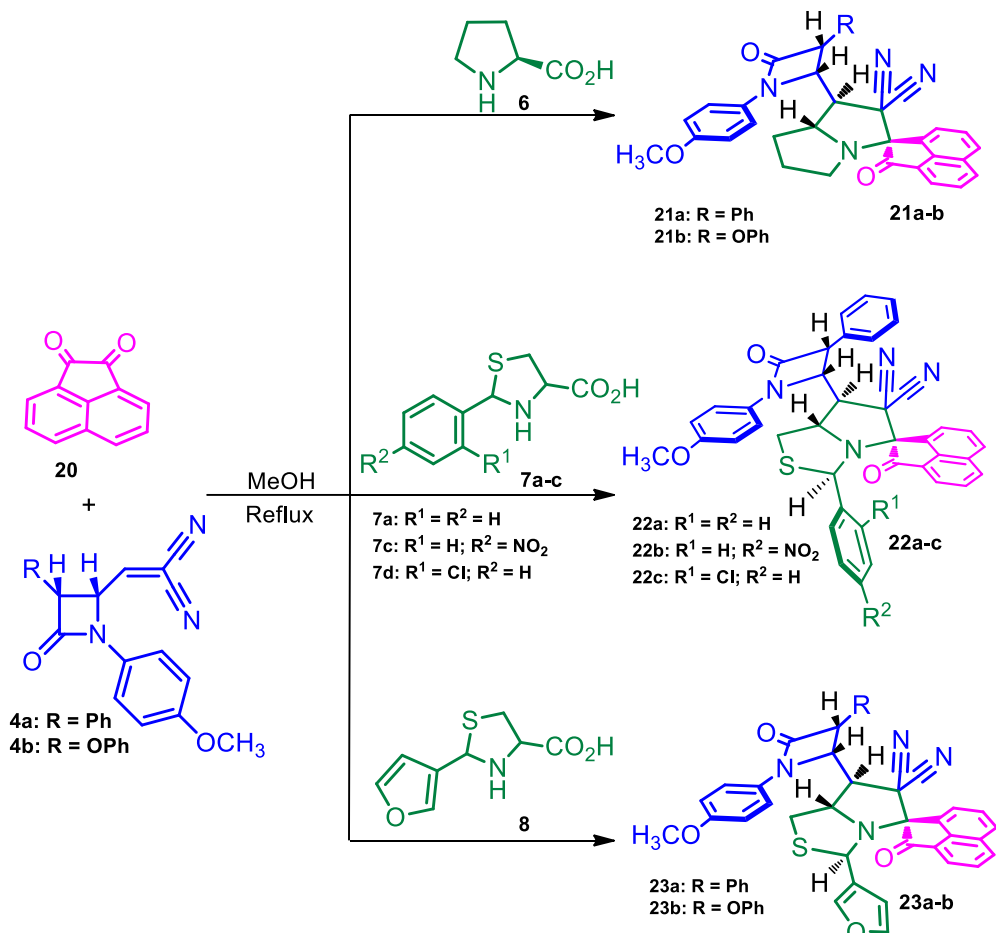
In conclusion, a facile synthesis of structurally diverse novel  $\beta$ -lactam embedded spiropyrrolizidines/pyrrolothiazole heterocyclic hybrids has been achieved via regio- and stereoselective three component 1,3-dipolar cycloaddition of azomethine ylide generated *in situ* from non-enolizable diketones and L-proline/ substituted thiaproline with  $\beta$ -lactam dipolarophiles. To the best of our knowledge,  $\beta$ -lactam containing gem-dicyano olefinic segment was utilized as the dipolarophile in cycloaddition reaction for the first time. Further, the cycloaddition strategy provided up to five stereogenic carbons including a spiro and a quaternary carbon via the formation of two C–C and one C–N bonds in a single synthetic operation.

## 4. Experiment section

### 4.1. General considerations

All melting points are uncorrected.  $^1\text{H}$  NMR and  $^{13}\text{C}$  NMR spectra were recorded on BRUKER 300 MHz instrument in  $\text{CDCl}_3$  solvent with TMS as a standard. Chemical shifts are given in parts per million (d scale), and coupling constants are given in Hertz. Mass spectra were recorded on JEOL-DX303 HF mass spectrometer. Elemental analysis was carried out using PerkinElmer CHNS 2400B instrument. Single crystal X-ray diffraction analysis was performed using Endraf-Nonius CHD4 diffractometer and Bruker SMART APEX II detector diffractometer. Column chromatography was performed on silica gel (ACME, 100–200 mesh). Routine monitoring of the reaction was done using thin layer chromatography developed on

Scheme 3. Feasible mechanism for the formation of  $\beta$ -lactam grafted spiroheterocycles



**Scheme 4.** Synthesis of structurally diverse  $\beta$ -lactam tethered spiroacenaphthepyrrolizidine/pyrrolothiazole heterocyclic hybrids.

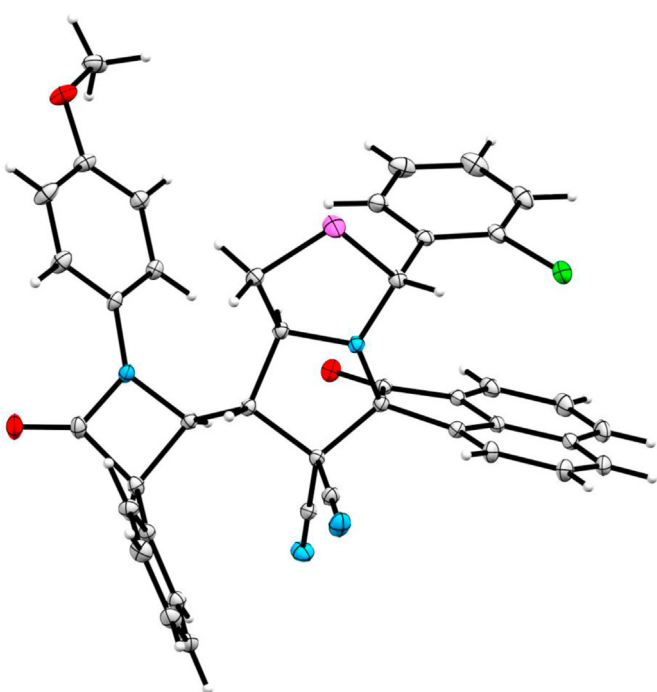


**Fig. 4.** X-ray structure of compound 22c.

glass plates coated with silica gel-G (ACME) of 25 mm thickness and visualized with iodine.

#### 4.2. General procedure for the preparation of 2-((1-(4-methoxyphenyl)-4-oxo-3-arylazetidin-2-yl)methylene) malononitrile

The 2-((1-(4-methoxyphenyl)-4-oxo-3-arylazetidin-2-yl)methylene) malononitrile **4a** was obtained by the reaction of 4-oxoazetidine-2-carbaldehyde **1a** (500 mg, 1.78 mmol) with malononitrile **2** (129 mg, 1.95 mmol) in a 1:4 mixture of water and ethanol (15 ml) in the presence of diisopropylamine **3** (0.05 ml) at 20 °C to room temperature for 1 h. The crystals that separated were filtered off and crystallized from a 1:2 mixture of ethyl acetate and hexane. The similar reaction protocol was applied for the synthesis of **4b**.

**2-((1-(4-Methoxyphenyl)-4-oxo-3-phenylazetidin-2-yl)methylene) malononitrile 4a:** Pale yellow solid; (75%), mp: 140–142 °C. <sup>1</sup>H NMR (300 MHz, CDCl<sub>3</sub>):  $\delta$  3.81 (s, 3H), 5.09–5.11 (d,  $J$  = 6.0 Hz, 1H), 5.25–5.30 (q,  $J$  = 6.0 Hz, 1H), 6.91–6.97 (m, 3H), 7.26–7.46 (m, 7H). <sup>13</sup>C NMR (75 MHz, CDCl<sub>3</sub>):  $\delta$  55.5, 55.9, 60.6, 93.2, 109.7, 110.5, 114.9, 118.0, 128.3, 129.1, 129.6, 130.0, 130.2, 157.2, 162.5, 165.2 ppm.

**2-((1-(4-Methoxyphenyl)-4-oxo-3-phenoxyazetidin-2-yl)methylene) malononitrile 4b:** Pale yellow solid; (82%), mp: 147–149 °C. <sup>1</sup>H NMR (300 MHz, CDCl<sub>3</sub>):  $\delta$  3.83 (s, 3H), 5.18–5.20 (d,  $J$  = 6.0 Hz, 1H), 5.31–5.36 (q,  $J$  = 6.0 Hz, 1H), 6.99–7.48 (m, 10H). <sup>13</sup>C NMR (75 MHz, CDCl<sub>3</sub>):  $\delta$  55.8, 56.1, 94.3, 99.7, 114.5, 114.9, 118.6, 121.1, 129.3, 130.7, 133.2, 157.7, 163.0, 166.6 ppm.

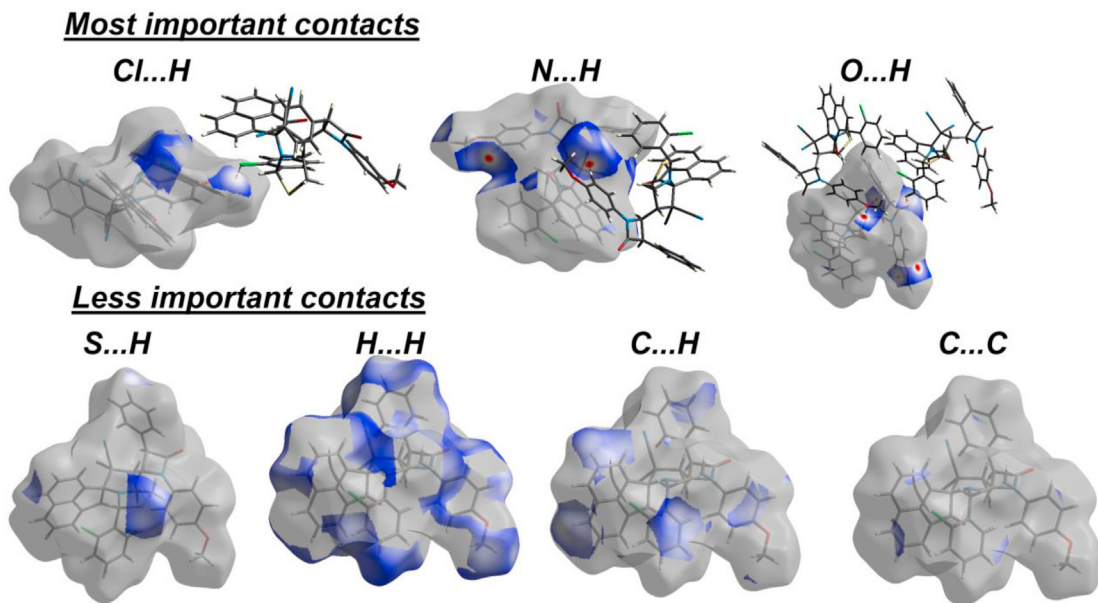


**Fig. 5.** Decomposed  $d_{\text{norm}}$  maps of most common contacts in the crystal structure of **22c**. Red, white and blue indicated shorter, equal and longer distance than van der Waals radii sum of the interacting elements.

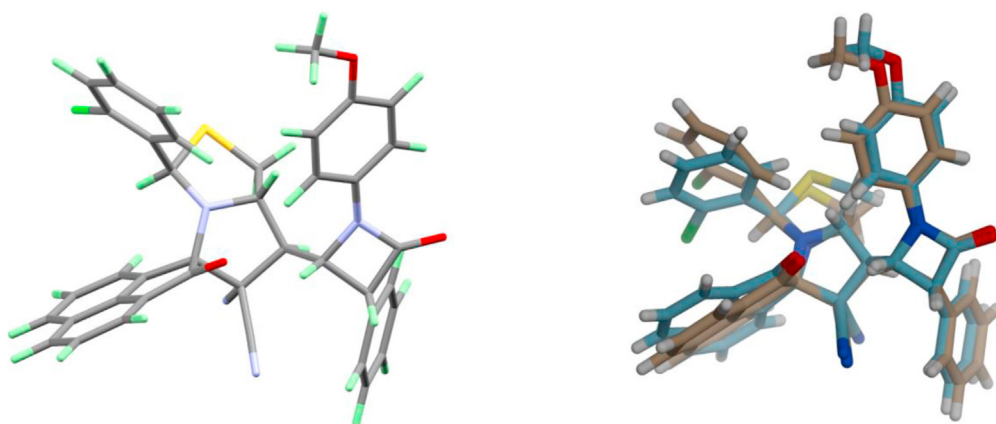


**Fig. 6.** The optimized geometry (left) and overlay of the optimized with experimental structures, (right) for compound **22c**.

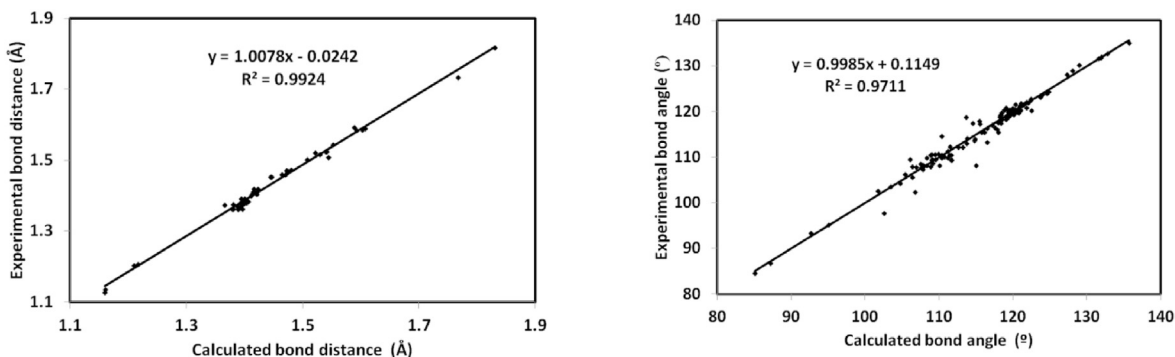


**Fig. 7.** The straight line correlations between the calculated and experimental geometric parameters.







- (1987) 649;  
 (b) I. Ojima, *Acc. Chem. Res.* 28 (1995) 383;  
 (c) I. Ojima, in: A. Hassner (Ed.), *Advances in Asymmetric Synthesis*, JAI, Greenwich, CT, 1995, p. 95;  
 (d) I. Ojima, F. Delaloge, *Chem. Soc. Rev.* 26 (1997) 377.
- [26] (a) A.R. Deshmukh, B.M. Bhawal, D. Krishnaswamy, V.V. Govande, B.A. Shinkre, A. Jayanthi, *Curr. Med. Chem.* 11 (2004) 1889;  
 (b) B. Alcaide, P. Almendros, *Curr. Med. Chem.* 11 (2004) 1921;  
 (c) C. Palomo, J.M. Aizpurua, I. Ganboa, M. Oiarbide, *Curr. Med. Chem.* 11 (2004) 1837;  
 (d) I. Ojima, L. Kuznetsova, I.M. Ungureanu, A. Pepe, I. Zanardi, J. Chen, in: V. Soloshonok (Ed.), *Fluorinecontaining Synthons, ACS Symposium Series*, vol. 911, American University Chemical Society/Oxford Press, Washington, DC, 2005, p. 544.
- [27] a) A.S. Kende, K. Liu, I. Kaldor, G. Dorey, K. Koch, *J. Am. Chem. Soc.* 117 (1995) 8258;  
 b) A. Chen, A. Nelson, N. Tanikkul, E.J. Thomas, *Tetrahedron Lett.* 42 (2001) 1251;  
 c) C.T. Brain, A. Chen, A. Nelson, N. Tanikkul, E.J. Thomas, *Tetrahedron Lett.* 42 (2001) 1247.
- [28] a) T.C. Boge, G.I. Georg, in: E. Juaristi (Ed.), *Enantioselective Synthesis of  $\beta$ -Amino Acids*, vol. 1, Wiley-VCH, New York, 1997, pp. 1–43;  
 b) C. Palomo, J.M. Aizpurua, I. Ganboa, M. Oiarbide, *Curr. Med. Chem.* 11 (2004) 1837;  
 c) A.R.A.S. Deshmukh, B.M. Bhawal, D. Krishnaswamy, V.V. Govande, B.A. Shinkre, A. Jayanthi, *Curr. Med. Chem.* 11 (2004) 1889.
- [29] N. Arumugam, R. Raghunathan, *Tetrahedron* 66 (2010) 969;  
 b) N. Arumugam, G. Periyasami, R. Raghunathan, S. Kamalraj, J. Muthumary, *Eur. J. Med. Chem.* 46 (2011) 600.
- [30] R. Rajesh, R. Raghunathan, *Eur. J. Org. Chem.* 2013 (2013) 2597.
- [31] R. Rajesh, M. Suresh, R. Raghunathan, *Tetrahedron Lett.* 55 (2014) 699–705;
- b) R. Rajesh, R. Raghunathan, *Synlett* (2013) 2107.
- [32] B. Alcaide, Y. Martin-Cantalejo, J. Perez-Castells, J. Rodriguez-Lopez, M.A. Sierra, A. Monge, V. Perez-Garcia, *J. Org. Chem.* 57 (1992) 5921.
- [33] D.S. Karthiga, T. Srinivasan, R. Rajesh, R. Raghunathan, D. Velmurugan, *Acta Crystallogr E69* (2013) o750.
- [34] D.S. Karthiga, T. Srinivasan, R. Rajesh, R. Raghunathan, D. Velmurugan, *Int. J. Chem. Res. 6* (2014) 2909.
- [35] M.J. Turner, J.J. McKinnon, S.K. Wolff, D.J. Grimwood, P.R. Spackman, D. Jayatilaka, M.A. Spackman, *Crystal Explorer 17*, University of Western Australia, 2017. <http://hirshfeldsurface.net>.
- [36] a) M.J. Frisch, G.W. Trucks, H.B. Schlegel, G.E. Scuseria, M.A. Robb, J.R. Cheeseman, G. Scalmani, V. Barone, B. Mennucci, G.A. Petersson, et al., *GAUSSIAN 09; Revision A02*, Gaussian Inc., Wallingford, CT, USA, 2009;  
 b) Gauss View, Version 4.1.2, in: R. Dennington II, T. Keith, J. Millam (Eds.), Semichem Inc., Shawnee Mission, KS, USA, 2007.
- [37] A.E. Reed, L.A. Curtiss, F. Weinhold, *Chem. Rev.* 88 (1988) 899..
- [38] J.I. Hubert, I. Kostova, C. Ravikumar, M. Amalanathan, S.C. Pinzaru, J. Raman Spectrosc. 40 (2009) 1033.
- [39] S. Sebastian, N. Sundaraganesan, *Spectrochim. Acta Part A Mol. Biomol. Spectrosc.* 75 (2010) 941.